THEORETICAL AND EXPERIMENTAL STUDY OF A SMALL UNIT FOR WATER DESALINATION USING SOLAR ENERGY AND FLASHING PROCESS

A. Safwat Nafey[a,*], M. A. Mohamad[b], S.O. El-Helaby[a], and M. A. Sharaf[a]

[a] Dept. of Engineering Science, Faculty of Petroleum and Mining Engineering, Suez Canal University, Suez, Egypt
[*] Tel.:+20-62-3303560; Fax: 20-62-3366252, E-mail: swazy20@hotmail.com
[b] Solar Energy Department, National Research Center, Cairo, Egypt

ABSTRACT

A small unit for water desalination by solar energy and flash evaporation process is investigated. The system is built at the Faculty of Petroleum and Mining Engineering at Suez-Egypt. The system consists of a solar water heater (flat plate solar collector) working as a brine heater, and a vertical flash unit which is attached with a condenser/preheater unit. In this work, the system is investigated theoretically and experimentally at different real environmental conditions along Julian days of one year. A mathematical model is developed to calculate the productivity of the system under different operating conditions. BIRD model for the calculation of solar insolation is used to predict the solar insolation instantaneously. Also the solar insolation is measured by a high sensitive digital pyranometer. Comparison between the theoretical and experimental results is performed. The system is tested during the summer and winter months. The average accumulative productivity of the system in November, December and January raged between 2.5 to 3.5 kg/day. The average summer productivity ranged between 13 to 16 kg/day in July and August and 10 to 12 kg/day in June.

Keywords: Desalination; Flash unit; Solar water heater; Solar energy

INTRODUCTION

Global resources of fresh water are scarce, unevenly distributed and, in many cases, may require some form of treatment and handling. These limited resources have resulted in water shortages in 88 developing countries across the world containing 50% of the world's population [1]. Need for purification of saline water is increasing due to an increase of population and limited supply of potable water.

Using solar energy is a practical method for obtaining small amounts of fresh water from saline water. Solar water distillation has been a subject of great interest for several decades [2]. The standard techniques like multi stage flash, multi effect distillation, vapor compression and reverse osmosis are reliable for large capacity

range of (100-50,000) m^3/day of fresh water production. However, these technologies are expensive for small amounts of fresh water. Moreover, they can not be used in locations where there are limited maintenance facilities. In addition, the use of conventional energy sources to drive these technologies has a negative impact on environment [3]. Solar desalination techniques are considered to be clean operations for producing clean water from the saline water. Also techniques of solar desalination are many and varying according to the size of the demanding of fresh water and the sizing of solar energy presence. El-Nashar presents a small solar Multi Effect Distillation (MED) of seawater desalination processes for remote arid areas [4]. A solar stand-alone system consisting of a Multi-Effect Stack (MES) evaporator supplied by thermal energy from flat plate or evacuated tube collectors with pumping power supplied by a solar PV system was investigated [5]. Lourdes Garcia-Rodriguez presented a preliminary design for different solar systems of seawater distillation processes. The solar collectors were parabolic trough ones in which brine circulate as thermal fluid. Steam is directly obtained from circulating brine. The solar collector field could be connected to condenser/preheater heat exchangers; nevertheless, the system would have a low performance ratio. Nafey et al [6] presented a small size of solar still unit that could be suitable for small groups of people. In that work, four experimental still units of 0.25 m^2 each are constructed. The maximum accumulative productivity of the still was about 10 lit/day. Also Soliman et al [3] examined a humidification dehumidification desalination system powered by solar collector with total unit productivity equal to 5 kg/day. Multi-stage flash (MSF) plants represent one of many other solutions to overcome the problem of water shortage. Actually, a small range of top brine temperature beginning from 50ºC can operate MSF processes. Solar stills, solar ponds and solar collectors can produce these small ranges of temperatures needed in flashing process. Kriesi [7] constructed a conventional 6 m^3/day MSF plant with a brine maximum temperature of 120ºC and coupled with a concentrating solar greenhouse collector and a hot water storage tank. Also; scheme for large-scale desalination of seawater by solar energy and MSF process was manufactured in Thar Desert of India [8]. The scheme was designed to produce about 5.25×10^7 m^3/year of fresh water with 11.52 km^2 of collector area. Ziad M et al [9] presented a single flash unit powered by a flat plate solar collector. The maximum allowable top brine temperature was ranged between 50-70ºC. However, the process is still in needs for more theoretical and experimental investigation. In the present work a small size of flash unit is used with the solar energy for producing a small amount of potable water. This system is operated and investigated at the Faculty of Petroleum and Mining Engineering at Suez-Egypt. The system is mainly consists of a flat plate solar collector (FPC) and a flash evaporation unit. The system is operated and investigated under real environmental conditions during winter and summer seasons. Generally, the total productivity of the system in winter ranged between 2.5 to 3.5 kg/day, and the summer productivity ranged between 10 to 16 kg/day. The main objective of this study is to perform a theoretical and experimental investigation of the process performance under real operating conditions.

SYSTEM DESCRIPTION AND EXPERIMENTAL WORK PROCEDURE

Figure 1 shows the system components. Simply the system containing: solar water heater (FPC) (1) and flash evaporation unit (2) designed vertically and attached to the condenser/preheater unit (3). Feed water enters the condenser inlet point (4) at a known temperature then passing through the condenser tubes till out going from the outlet point (5) with a new temperature value caused by the heat transferred from the vapor that condensate across the outside surface of the condenser tubes. Then feed water enters the solar collector with its new temperature to raise it to the top brine temperature (TBT) before entering the flash chamber. Then hot seawater enters the flash chamber by passing through a brine injector (6). The seawater injector is operated at maximum flow rate equal to 1.4 lit/min and minimum flow rate equal to 0.8 lit/min. The wasted brine then exits after releasing its vapor (7) that condensates on the condenser tubes (8) to produce fresh water.

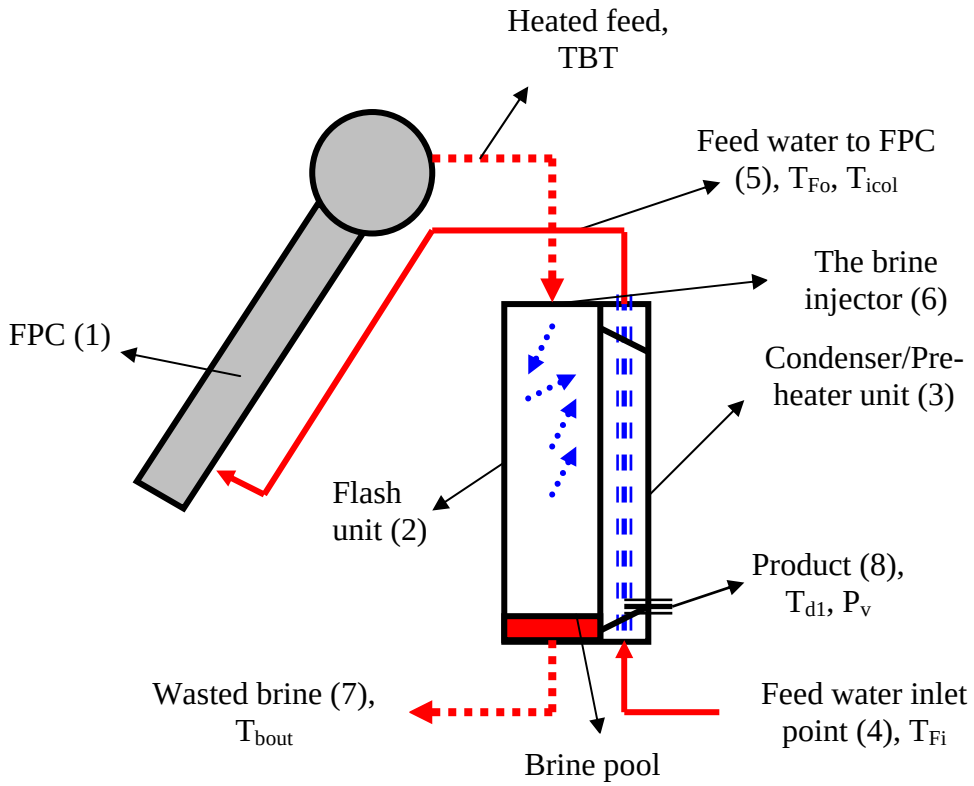

Figure (1) A schematic draw of the system components

1. Flash evaporation unit

Flash chamber is designed as a steel cylindrical tank coated with epoxy steel to prevent outside environmental corrosion effects and to reduce the thermal losses to the ambient. The height of the flash chamber is 1m, width diameter is 0.5m. The brine level is controlled to be 20cm in the flash tank. The tank weight is about 95 kg and its

thickness equal to 3mm. Fig. 2 shows the flash unit that attached to the condenser unit. Fig. 3 shows a photograph of the flash chamber without attaching to the condenser unit.

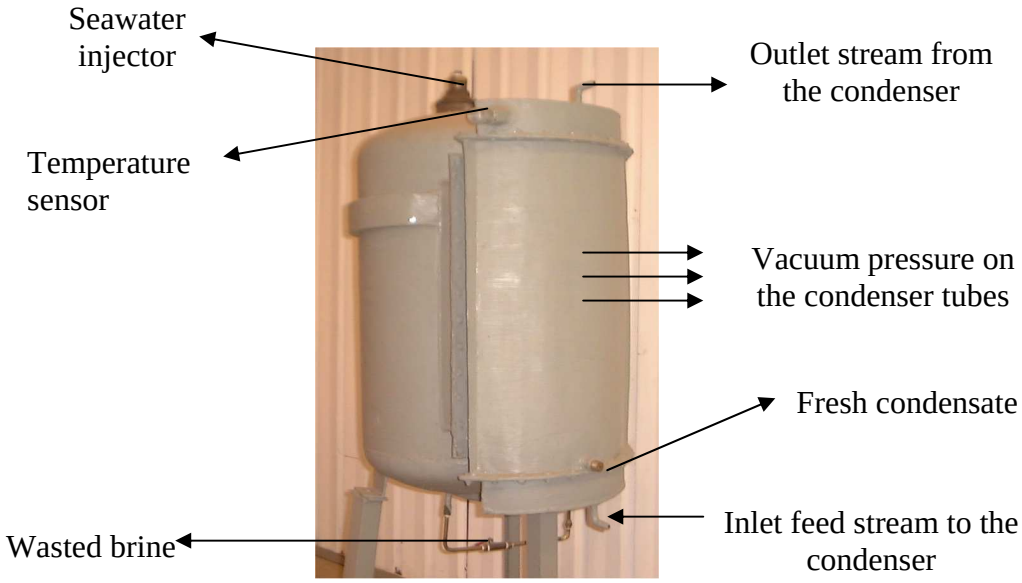

Figure (2) The photograph of the flash chamber attached to the condenser unit

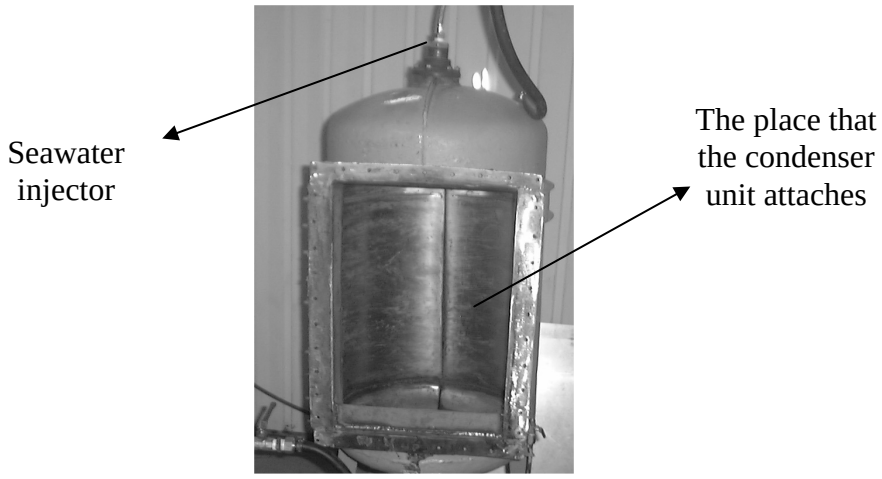

Figure (3) The flash chamber without its condenser

The hot seawater enters the flash chamber through the seawater injector at a pressure equal to 2.5 bar at maximum flow rate, and 1.5 bar at minimum flow rate. The injector is designed to control the feed water to the system by a control valve opening at three positions.

2. The condenser/preheater unit

The condenser unit is very important part in this system. The main parts of this unit are copper tubes, upper and lower headers and the outside cover. The tubes across the condenser unit are made from copper with thermal conductivity 387 W/m.K. The tube length is 65cm and the inner diameter is 0.8 cm and the outer diameter is 0.98cm. The number of tubes is 69 tubes to perform a total length of about 45m and total condenser area equal to 1.388 m^2. Every tube bank contains 5 tubes staggered distribution. The tubes are welded at their ends by an epoxy steel welding material in a flange made of steel copper to prevent leakages. To fix the condenser to the flash unit without any leakages; a rubber frame is welded to the condenser. Fig. 4 shows a photograph of the condenser at different views with its inside tubes without covering or headers.

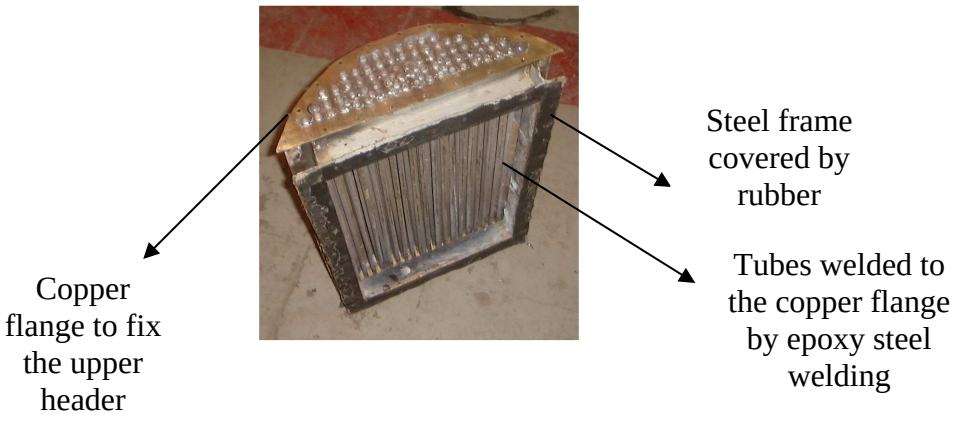

Figure (4) Different views of the condenser unit with its tubes

3. Solar collector (brine heater)

The brine heater in this work is a flat plate solar collector. The collector is manufactured by Solar Energy Corporation Foundation at Egypt-Cairo. The collector technical data are listed in Table 1.

The collector is operated with a slope angle 45^o. The collector aspects degree is 180^o south. The connections tubes between the collector and the flashing unit are made of plastic material and insulated by reflectance material. The tubes are made of plastic to reduce thermal losses to the ambient. The diameter of the plastic tubes is ¾ inch. The position of the collector is 3 m above the flashing unit.

Table 1. The manufactured characteristics of the collector

Absorber material:	Aluminum plate thickness=0.5mm
Collector area:	Ac=2.39m^2
Absorber area:	Ap=2.1m^2
Effective area:	A_e=88% of the collector area
Coating absorptance:	92%
Coating emittance:	15%
Glass cover transmittance:	91%
Insulation thickness:	37mm
Absorber thickness:	Aluminum steel=0.5mm
Glass cover thickness:	3mm
Collector weight:	58,5 kg
Tube risers mean diameter:	16mm
Tube headers mean diameters:	28mm
Tube spacing across the collector:	S_t=16.3cm
Risers tube length:	1.81m
The plate to glass cover spacing:	70mm
Number of glass cover:	1

Where ***Ac*** is the collector total area, ***Ap*** is the plate heat transfer area, A_e is the collector effective area, S_t is the tube spacing.

MEASUREMENTS OF THE EXPERIMENTAL DATA

1. Temperature

The different temperatures of the system (see Fig. 1) are measured by a digital volt meter through signals provided by number of thermocouples. The device relative error is less than 1%. The ambient temperature is measured by a common glass-tube-mercury temperature meter.

2. Solar radiation and wind velocity

Solar radiation is measured by a solar radiation pyranometer laid on the collector surface with slope angle equal to 45^o. The error of the device is about 3%. An anemometer is used to measure the wind speed in m/s.

3. Pressure

The inlet feed water and vacuum pressures are measured by pressure sensors. The pressure sensor for the inlet feed water is put directly after the brine injector valve. The vacuum pressure sensor is put at distillate outlet valve.

CONDENSATE AND WASTED BRINE FLOW RATES

By collecting the condensate and outlet wasted brine in two calibrated tanks at a certain time, the flow rate of both the condensate and brine can be measured.

MATHEMATICAL MODEL

The process mathematical model consists of two parts. The first part is for estimating the solar intensity. Seven different models are statistically examined by comparing the measured and calculated values of the solar intensity [16]. BIRD's model [10] gives the more matched results for Suez-Gulf area. The second part contains the equations representing the process units. Using the measured values of solar intensity, wind velocity, ambient temperature and all operating parameters (temperatures and pressures), the daily productivity of the system can be calculated by the developed program.

1. The mathematical model of the process units

The second part of the mathematical model is representing the flat plate solar collector and the flashing unit with its condenser.

1.a. Mathematical model for the flat plate solar collector

The energy balance equation of the solar collector can be written as follows [11];

$$I_S \times A_c = Q_{loss} + Q_u + Q_{stg} \quad (1)$$

Where I_S is the energy from the sun, A_c is the collector effective area, Q_{loss} is the heat loss from the collector and Q_u is the useful energy transferred from the absorber to the flash chamber and Q_{stg} is the energy stored in the collector. The heat loss is expressed by Frederick [12] as;

$$Q_{loss} = A_c U_l F'(\overline{T}_f - T_{amb}) \quad (2)$$

The overall heat loss of the collector U_l is the summation of three components; the top loss U_t, the bottom loss U_b, and the edge loss U_e and the other variables are defined in the nomenclature.

$$U_l = U_t + U_b + U_e \quad (3)$$

Where, the bottom and edge losses are calculated respectively as following [15]:

$$U_b = k_b / l_b \quad (4)$$

$$U_e = (k_e / l_e) \times \frac{2(C_L + C_W)C_h}{C_L \times C_W} \tag{5}$$

An empirical equation for the top losses U_t for both hand and computer calculations was developed by Klein (1975) [13].

$$U_t = \left[\frac{NG}{\frac{C}{T_{mp}}\left[\frac{(T_{mp} - T_{amb})}{(NG + f)}\right]^e + \frac{1}{h_w}} \right]^{-1} + \frac{\sigma(T_{mp} + T_{amb})(T_{mp}^2 + T_{amb}^2)}{(\varepsilon_p + 0.00591NG \times h_w)^{-1} + \frac{2NG + f - 1 + 0.133 \times \varepsilon_p}{\varepsilon_g} - NG} \tag{6}$$

Where,
NG is the number of glass covers, $f = (1 + 0.089h_w - 0.1166h_w\varepsilon_p)(1 + 0.07866NG)$, $C = 520 \times (1 - 0.000051\beta^2)$ for $0^o < \beta < 70^o$, $e = 0.43(1 - 100 / T_{pm})$ where β is the collector tilt angle in degree and h_w is the wind heat transfer coefficient and given by [11] as;

$$h_w = 5.7 + 3.8 \times V_w \tag{7}$$

Efficiency factor $F^{'}$ of equation (2) can be calculated as follows;

$$F^{'} = \frac{\frac{1}{U_t}}{s\left(\frac{1}{U_t[(s_t - d)F + d]} + \frac{1}{\frac{kb}{l}} + \frac{1}{h_f \pi d_i} \right)} \tag{8}$$

The fin efficiency F is given by; [11]

$$F = \frac{\tanh\left[\sqrt{\frac{U_t}{k\delta}}\left(\frac{s_t - d}{2}\right)\right]}{\sqrt{\frac{U_t}{k\delta}}\left(\frac{s_t - d}{2}\right)} \tag{9}$$

The heat removal factor is calculated from; [11]

$$F_R = F' \times \frac{GC_p}{U_t F'} \left(1 - \exp - \left(\frac{U_t F'}{GC_p}\right)\right) \tag{10}$$

Where $G=m/A_c$. Once F_R is calculated, the useful energy from the collector can be calculated from the following equation;

$$Q_u = F_R A_c [I_s - U_l (T_{icol} - T_{amb})] \tag{11}$$

The energy stored is expressed by Frederick [12] as;

$$Q_{stg} = A_c C_c \frac{d\overline{T}_{col}}{dt} \tag{12}$$

1.b. Mathematical model for the flashing unit

Fig. 5 shows the flashing unit with its stream variables [14].

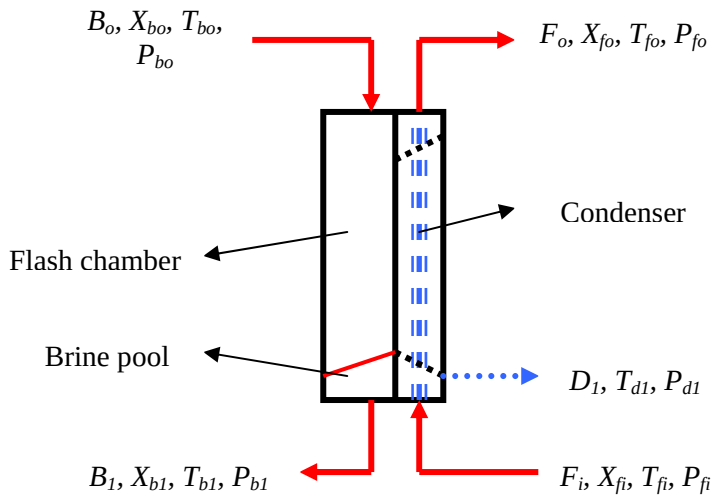

Figure (5) A flash stage unit.

The energy balance for the flashing brine is expressed as follows,

$$B_o^{\cdot} h_o (T_{bo}, x_{bo}) = B_1^{\cdot} h_{b1} (T_{b1}, x_{b1}) + [(B_o^{\cdot} - B_1^{\cdot}) H_{V1} (T_{b1}, P(T_o))] \tag{13}$$

Where,

$$B_1^{\cdot} = W_{b1} + X_{b1} \tag{14}$$

Equations (15) and (16) below shows the overall mass balance for both flash and condenser units,

$$B_o^{\cdot} = D_1^{\cdot} + B_1^{\cdot} \tag{15}$$

$$F_i^{\cdot} = F_o^{\cdot} \tag{16}$$

And the flash unit enthalpy balance is;

$$\dot{B}_o h_o + \dot{F}_i h_{Fi} = \dot{B}_1 h_{b1} + \dot{D}_1 h_{D1} + \dot{F}_o h_{Fo} + Q_{loss} \tag{17}$$

While the overall heat transfer coefficient is represented by the following equation [14],

$$U_1 = f(\phi, T_{Fi}, T_{Fo}, T_{D1}, ID_1, OD_o, FF, R_F) \tag{18}$$

The amount of heat exchanges across the condenser heat transfer surface Q_1 is calculated by equation (19),

$$Q_1 = \dot{m}_{Fi,o} c_p (T_{Fo} - T_{Fi}) = U_1 A_1 \times \Delta T_{lm1} \tag{19}$$

From equation (19),

$$\frac{U_1 \times A_1}{\dot{m}_{Fi,o} c_p} = \ln \frac{T_{D1} - T_{Fi}}{T_{D1} - T_{F0}} = -\ln \frac{T_{D1} - T_{F0}}{T_{D1} - T_{Fi}} \tag{20}$$

From equation (20), the following equation is obtained:

$$(1-E) \times T_{Fi} + E \times T_{D1} - T_{Fo} = 0 \tag{21}$$

Where $E = 1 - e^{-NTU_1}$ and $NTU_1 = U_1 \times A_1 / \dot{m}_{Fi,o} c_p$

$$T_{D1} = T_{b1} - NEA - BPR \tag{22}$$

The non-equilibrium allowance *NEA* and *BPR* are calculated by the following equations [14],

$$NEA = A + B \times T_{b1} + C \times T_{b1}^2 + D \times T_{b1}^3 \tag{23}$$

$$BPR = (B + C \times X) \times X \tag{24}$$

Where,

$$10^3 \times B = 6.71 + 6.43 \times 10^{-2} \times T_{b1} + 9.74 \times 10^{-5} \times T_{b1}^2$$

$$10^5 \times C = 2.38 + 9.59 \times 10^{-3} \times T_{b1} + 9.42 \times 10^{-5} \times T_{b1}^2$$

Using the measured values of solar intensity, wind velocity and ambient temperature as input data, the daily productivity of the system can be calculated. The average values for climatic conditions such as ambient temperature, inlet seawater temperature, wind speed and solar intensity are taken during the day hours. Using these conditions, with initializing the unknown temperatures; the system units' heat transfer coefficients are calculated. With a reasonable specific tolerance, the mathematical model is solved by Gauss-Seidel iteration method.

RESULTS AND COMMENTS

For illustration the detailed results for just two days (one during the summer season and the other during the winter) are considered in the following sections.

1. Summer results

The measured data and parameters obtained on the 9th June, 2005 are illustrated in Tables 2 and 3. Feed water flow rate is considered to be constant and equals to 0.0183 kg/s. During the operating hours, the system goes under steady state conditions. Losses from the flash unit to the ambient are neglected.

Table 2 Measured weather conditions and results on a Julian day 160 in June 2005

Time	**-**	**9**	**10**	**11**	**12**	**13**	**14**	**15**	**16**	**hr**
Is	-	450	562	650	680	648	571	474	415	**W/m^2**
T_{amb}	-	26	27	28	29	30	30	31	30	**^{o}C**
V_w	1.3									**m/s**
T_{Fi}	27									**^{o}C**
T_{Fo}	-	31	36	38	39	37	36	36	36	**^{o}C**
TBT	-	50	52	54	56	52	50	50	49	**^{o}C**
T_{b1}	-	37	39	41	42	40	39	39	37	**^{o}C**
T_{d1}	-	32	37	39	40	38	37	37	36	**^{o}C**
T_g	-	33	33	34	35	34	34	33	33	**^{o}C**
T_{icol}	-	31	36	38	39	37	36	36	36	**^{o}C**
T_{ocol}	-	50	52	54	56	52	50	60	59	**^{o}C**
PR	-	0.7	0.85	0.8	0.9	0.8	0.8	0.9	0.9	-
T_{ins}	31									**^{o}C**
Fs	0.0183									**kg/s**
Product	11									**kg/day**

Table 3 The estimated energy values through the solar collector on a Julian day 160 in June 2005

Q_{stg}	-	0.02	0.62	1.34	1.65	1.39	0.71	0.13	0	**W/m^2**
Q_{loss}	-	64.52	78.73	89.55	91.37	80.89	69.86	56.68	50.87	**W/m^2**
Q_u	-	385.4	482.6	559.09	587.01	565.7	500.4	417.18	364.22	**W/m^2**
U_{loss}		3.98	3.91	4.01	4.04	4.05	4.03	4.02	4.02	**W/m^{2}K**
U_{tloss}	-	2.26	2.31	2.35	2.38	2.39	2.37	2.36	2.36	**W/m^{2}K**
U_{eloss}	0.309									**W/m^{2}K**
U_{bloss}	1.35									**W/m^{2}K**
Efficiency Factor	0.93									
Heat Removal Factor	0.88									

The measured data show that the system productivity is 11 kg/day. For 9th June, 2005 the average total solar irradiance obtained on the collector surface is about 4.45 $kWhr/m^2$. Fig. 6 shows the hourly variation in solar radiation during the 9th of June, 2005. The mean values of the fractional percentage error between the theoretical and the experimental results; about 2% (see Table A-1). Fig. 7 shows the characteristic efficiency and operating temperatures curves of the collector (brine heater). Fig. 7 gives a clear aspect about the collector ranking to any other collectors due to the efficiency factor and heat removal factors values. Figs. 8 to 10 show the experimental and theoretical results of the system operation during the 9th of June. Fig. 8 represents the temperature distribution of the system during the day operation. The temperatures increase gradually due to the changing in solar intensity along the day operation. Theoretical and experimental results for the temperatures distributions are in a good agreement as shown in Fig. 8.

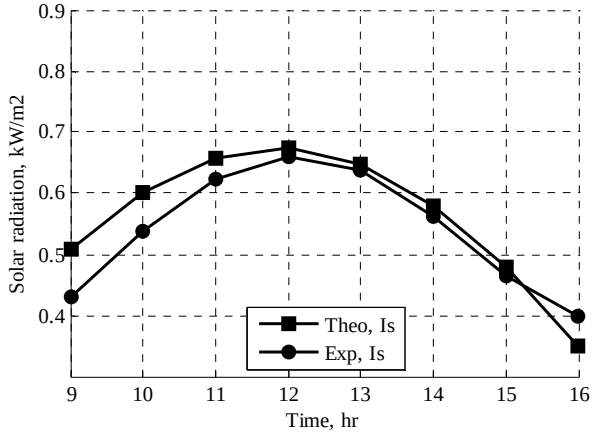

Figure (6) The hourly variation in solar radiation during the 9th of June 2005

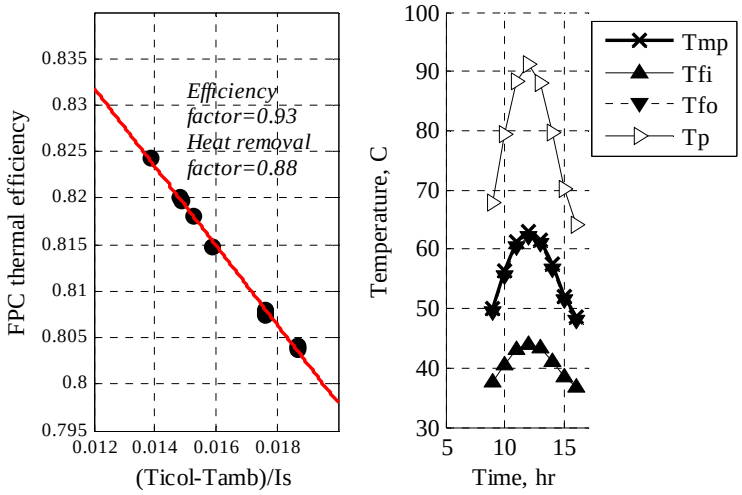

Figure (7) The characteristic efficiency and operating temperatures curves of the collector (brine heater)

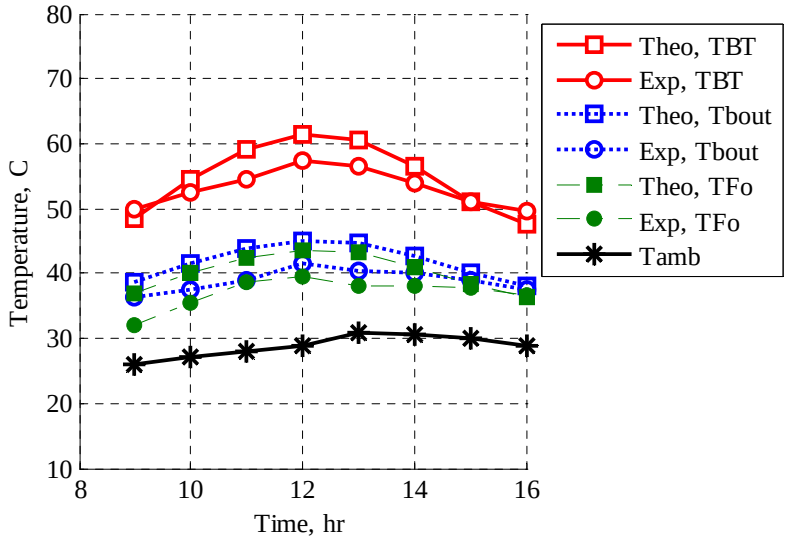

Figure (8) The temperature distribution of the system along the day operation during the 9th of June 2005

The performance ratio can be estimated as follows:

$$PR_n = \frac{\sum_{1...n} D_{tn}^{\cdot} \times Hv_n}{I_S \times Ac} \qquad (25)$$

where I_S is the solar intensity in kW/m^2 and A_c is the collector heat transfer area in m^2, Hv_n is the latent heat of vaporization at stage (n), $D_{tn}^{\cdot}$ is the rate of total productivity at stage (n). The stage temperature drop, ΔT_{st} is equal to the difference between TBT and the wasted blow down brine T_{b1}, and is known as the flashing range. Fig. 9 shows the hourly variations in the system performance ratio (PR) and the flashing range ΔT_{st}. The figure shows that the PR is ranged between 0.8-0.9 and ΔT_{st} is ranged between 11-15^{o}C.

Figure 10 shows the system hourly productivity on the same day in June. The accumulative productivity on this day is about 11 kg/day. Also, the figure shows that the top value of distillate product (DP) obtained were about 1.75 kg/hr.

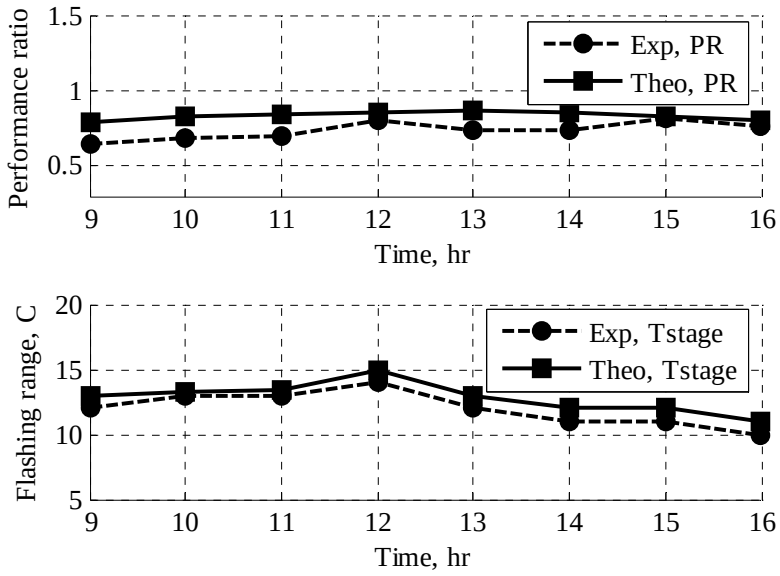

Figure (9) The system performance ratio and the system flashing range during the 9th of June 2005

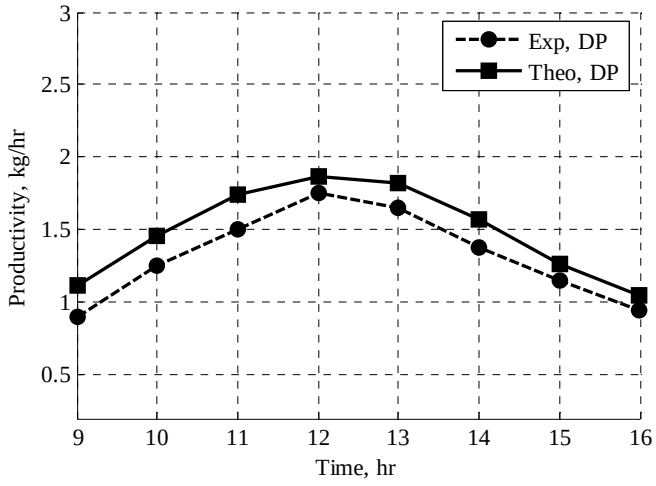

Figure (10) The hourly productivity of the system during the 9th of June 2005

2. Winter results

Table 4 shows the measured data on 21st January, 2005 as example of the winter conditions. The table shows that the productivity is 2.5 kg/day. The TBT is recorded as 38-42°C which is considered too low to drive the flashing operation. The maximum obtainable solar intensity on that day was 447 W/m^2. This value of the measured solar flux is weak to produce the suitable TBT. Generally the fresh water productivity and the performance ratio of the system are smaller in the winter operation than summer operation.

Table 4 Measured weather conditions and results on a Julian day 21 in January 2005

Time	**9**	**10**	**11**	**12**	**13**	**14**	**15**	**16**	**17**	**hr**
Is	266	370	432	447	415	341	230	90	-	**W/m^2**
T_{amb}	17	18	22	23	22	21	20	19	17	**^{o}C**
V_w	1.5									**m/s**
T_{Fi}	18.5									**^{o}C**
T_{Fo}	22	25	27	28.5	26	25.5	23.5	21.5	-	**^{o}C**
TBT	38	39	40	42	41	41	40	39	-	**^{o}C**
T_{b1}	24.5	28	30	32	31	31	30	29	-	**^{o}C**
T_{d1}	22	25	27	28	26	25	23.5	21.5	-	**^{o}C**
T_g	22	23	25	25	23	23	22	21	-	**^{o}C**
T_{icol}	22	25	27	28.5	26	25.5	23.5	21.5	-	**^{o}C**
T_{ocol}	38	39	40	42	41	41	40	39	-	**^{o}C**
PR	0.6	.65	0.7	0.85	0.8	0.75	0.6	0.6	-	-
T_{ins}	21									**^{o}C**
Fs	0.0183									**kg/s**
Product	2.5									**kg/day**

Figure 11 shows the variations of the solar radiation on 21st January, 2005. The figure illustrates the agreement between the theoretical model results of solar radiation (BIRD model) and the measured results that the maximum error is 2%. Figure 12 shows the system temperature distribution along the day operation hours. It is seen from Fig. 12 that the temperatures are increasing gradually till the mid day and then decrease gradually till the shut off operation at the end of the day light hours. Also the figure shows a good matching between the theoretical and experimental results for this day. Figure 13 shows both of the PR and the flashing range ΔT_{stg} . PR is not exceeding about 0.7 to 0.8 in winter, and ΔT_{st} is ranged from 10 to 12ºC. Figure 14 shows the hourly productivity of the system. The figure shows a comparison an acceptable different between the theoretical and measured results with an error about 9%. The total distillate productivity DP is not exceeding about 2.5 kg/day on 21st of January. The lower productivity in winter is caused by the lower solar intensity against summer value.

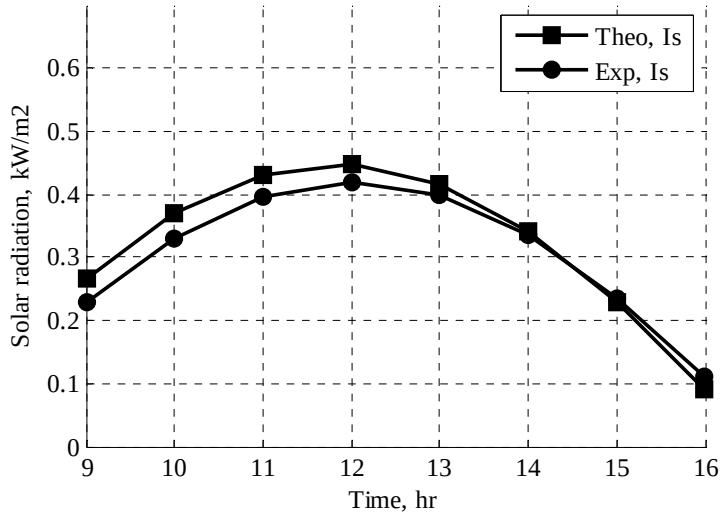

Figure (11) Variation of solar radiation with time during the 21st of January 2005

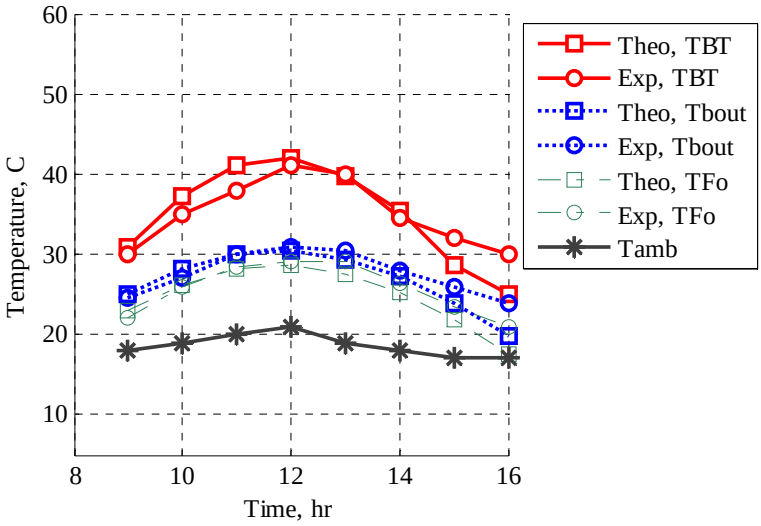

Figure (12) The temperature distribution of the system during the 21st of January 2005

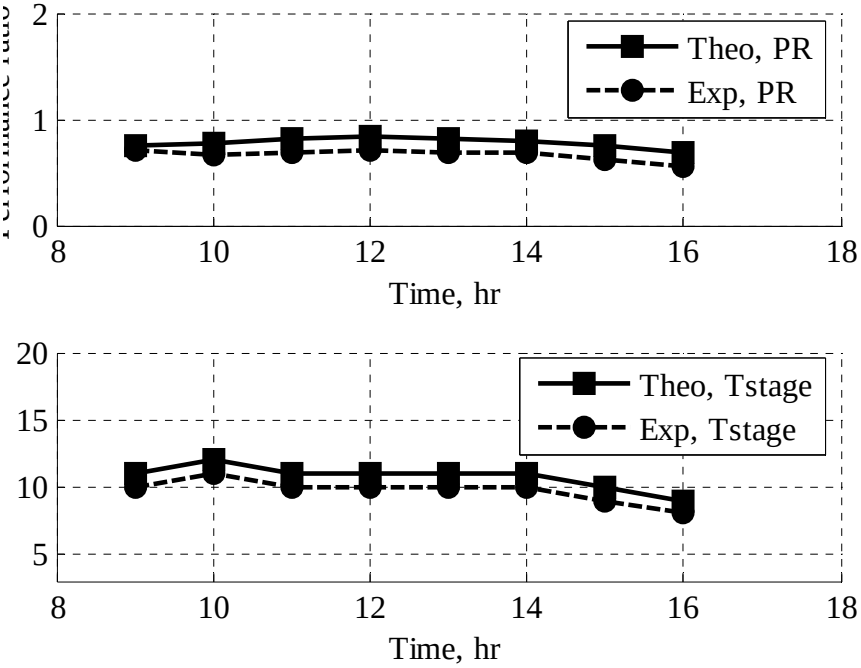

Figure (13) The system unit performance ratio and the system flashing range during the 21st of January 2005

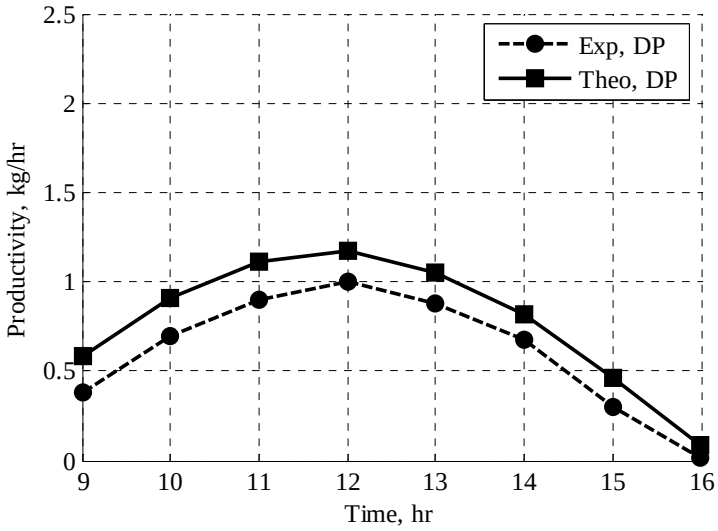

Figure (14) The hourly productivity of the system during the 21st of January 2005

Following the same sequence for the days of one year long, the average measured data and results are tabled in Table 5 below.

Table 5 The average values obtained for the system operation along one year

Month	T_{Fi} °C	T_{Fo} °C	TBT °C	T_{b1} °C	I_S Whr/m^2	T_{amb} °C	T_g °C	T_{ins} °C	V_w m/s	Product kg/day
1/2005	18	25.125	40	26	3144	20	24	22	2.25	2.5
2/2005	19	25.357	44.25	28	3469	23	30	26	1.3	4.5
3/2005	20.25	28.125	48	34.5	4049	24	30.5	27	4.2	6.5
4/2005	22.6	32	49	35.5	4462	25	31	28.25	3.7	8
5/2005	24	34	52	36.5	4495	27.5	30	30	1.05	8.5
6/2005	27.25	36.125	53	40	4750	29	34	30.25	2.5	11
7/2005	27.6	38	60	44	4867	31	35	32.357	1.5	14
8/2005	28.75	39	67	43.75	5120	33	36.5	34.5	0.8	16.5
9/2004	26.75	36.5	52	42	4601	29	36.5	30.75	3.25	12
10/2004	26.5	35.25	49	37	3858	28	35.6	31	3.7	9
11/2004	20.375	34	44	35	2888	23	32	30	3.8	5
12/2004	17.125	32	42	34.5	2791	19	28.5	23.5	1.625	3.5

CONCLUSIONS

To summarize and conclude the results and the discussions in this article, the following points could be withdrawn:

1. A mathematical model is written for the all system components (collector, flash unit, condenser unit) to predict the system productivity under different and wide range of operating conditions.
2. The unit performance ratio is low because it ranged about 0.7 to 0.8 in winter and 0.8 to 0.9 in summer.
3. The system daily productivity in summer is about 10 to 16 kg/day, and about 2.5 to 3.5 kg/day during the winter season.
4. The *Fr* percentage error of the system performance ratio was not exceeding about 9% the total productivity DP.
5. The collector efficiency factor is about 0.93 and the heat removal factor is about 0.88.
6. The system works better at higher TBT, i.e., higher solar intensity. Reasonable rate of feeding water is ranged about 0.0183 kg/s.
7. The results of the proposed mathematical model are in good agreement with those of the experimental model of the system.

NOMENCLATURE

A Tends to area in m^2, or a parameter used in equation 22
A_1 Condenser heat transfer area (m^2)
A_c The collector heat transfer area (m^2)
A_e The collector effective area (m^2)
A_p The collector absorber area (m^2)
B Tends to the brine, or a parameter used in equation 23, 24

B_o Mass flow rate of the brine entering the flash unit (kg/s)
B_1 Mass flow rate of the brine exiting from the 1st flash unit (kg/s)
BPR Boiling point elevation of saline water parameter
b The thickness of the bond (m)
C Tends to the parameter used in equation 23, 24 or the collector heat capacity
C_p Bond conductance
C_h Collector height (m)
C_L Collector length (m)
C_W Collector width (m)
c_p Specific heat capacity of saline water (kJ/kgK)
D Tends to distillate or parameter used in equation 22
DP Distillate product kg/hr
D_1 Distillate product from the 1st stage (kg/s)
d Collector tube outer diameter (m)
E Parameter used in equation 20
F Fin efficiency
$F_{i,o}$ Inlet and outlet feed water to the condenser (kg/s)
FPC Flat plate collector
FF Flooding factor
F' Efficiency factor for solar collector
F_R Heat removal factor
F_S Feed water system (kg/s)
H_{v1} Latent heat of vaporization of water (kJ/kg)
h_f Fluid heat transfer coefficient (W/m^2K)
h_o Enthalpy stream of the inlet brine to the stage (W/m^2K)
h_{b1} Enthalpy stream of the outlet brine from the stage (kJ/kg)
h_{D1} Enthalpy stream of the distillate product (kJ/kg)
$h_{Fi,o}$ Enthalpy stream of the inlet and outlet feed water to the condenser (kJ/kg)
h_w Convection heat transfer coefficient (W/m^2K)
I_S Solar intensity (W/m^2)
ID_1 Inner diameter of the condenser tubes (m^2)
k_b Back insolation conductivity (W/mK)
k_e Edge insolation conductivity (W/mK)
k Thermal conductivity (W/mK)
l Length (m)
l_b Back insolation thickness (m)
l_e Edge insolation thickness (m)
$m_{Fi,o}$ Mass flow rate of feed water in and out of the condenser (kg/s)
NEA Non equilibrium allowance
NG No. of glass covers of the collector
NTU_1 No. of transfer unit parameter
OD_o Outer diameter of the condenser tubes (m^2)
P Tends to the pressure (kPa)
PR Unit performance ratio
P_{bo} Pressure stream of the inlet brine to the flash stage (kPa)
P_{b1} Pressure stream of the outlet brine from the flash stage (kPa)

P_{d1} Pressure stream of the distillate (kPa)
$P_{Fi,o}$ Pressure stream of the condenser (kPa)
Q_1 Thermal energy of the condenser in steady state (W)
Q_u Useful energy from the collector (W)
Q_{loss} Energy loss from the collector (W)
Q_{stg} Energy stored in the collector (W)
R_F Stage fouling factor
S_t Tube spacing (m)
TBT Top brine temperature (^oC)
T_o Top brine temperature (^oC)
T_{amb} Ambient temperature (^oC)
T_{bo} Inlet brine stream temperature to the flash stage (^oC)
T_{b1} Outlet brine stream temperature from the flash stage (^oC)
$T_{i,ocol}$ Inlet and outlet brine stream temperature to the collector (^oC)
$T_{D1,d1}$ Distillate product stream temperature (^oC)
$T_{Fi,o}$ Inlet and outlet feed temperature of the condenser (^oC)
T_g Collector glass cover temperature (^oC)
T_{ins} Collector insulation temperature (^oC)
T_{lm1} Logarithmic mean temperature (^oC)
T_{mp} Mean plate temperature of the collector (^oC)
T_p Plate temperature of the collector (^oC)
T_{v1} Vapor temperature (^oC)
U_1 Overall heat loss of the stage(W/m^2K)
U_t Overall top loss in the collector (W/m^2K)
U_l Overall losses in the collector (W/m^2K)
V_w Wind speed (m/s)
W_{b1} Flow rate of water in the brine (kg/s)
X Salt concentration
X_{b1} Flow rate of salt in the brine (kg/s)
β Collector tilt angle
σ Boltzmann constant
ε_g Emittance of glass cover
ε_p Emittance of absorber plate
δ Fin thickness (m)
ϕ Tube side brine velocity (m/s)

REFERENCES

[1] Hisham T. El-Dessouky, Hisham M. Ettouney, Yousef Al-Roumi, Multi-stage flash desalination: present and future outlook, Chemical Engineering Journal, Vol. 73, pp. 173-190, February 1999.

[2] Lianying Zhang, Hongfei Zheng, Yuyuan Wu, Experimental study on a horizontal tube falling film evaporation and closed circulation solar desalination system, Journal of Renewable Energy, Vol. 28, pp. 1187-1199, October 2003.

[3] Soliman, A., Study of Water Desalination by Solar Energy Using Humidification-Dehumidification Processes", Mech. Eng. Dep., Faculty of Petroleum & Mining Eng, Suez Canal Univ., M.Sc. Thesis, Egypt, 2002.

[4] Ali M. El-Nashar, The economic feasibility of small solar MED seawater desalination plants for remote arid areas, Journal of Desalination, Vol. 134, pp. 173-186, (2001).

[5] Lourdes Garcia-Rodriguez, Carlos Gomez-Camacho, Preliminary design and cost analysis of a solar distillation system, Journal of Desalination, Vol. 126, pp. 109-114.

[6] Nafey, A.S., Abdelkader, M., Abdelmotalip, A., Mabrouk, A.A., Enhancement of solar still productivity using floating perforated black plate, Journal of Energy Conversion & Management, Vol. 43, pp. 937-946, 2002.

[7] Kriesi, R., Design and operation experience with solar powered multistage desalination plants, Journal of Desalination, Vol. 39, pp. 109-116.

[8] Anil K. Rajvanshi, A scheme for large scale desalination of sea water by solar energy, Journal of Solar Energy, Vol. 24, pp. 551–560.

[9] Ziad, M., Badawi, W. Tleimat, Test results from a solar boiler for saline water distillation, Journal of Desalination, Vol. 39, pp. 63-70, 1981.

[10] Richard E. Bird, Roland L. Hulstrom, A simplified clear sky model for direct and diffuse insolation on horizontal surfaces, Journal of Solar Energy Research Institute, Golden, Colorado USA (1981).

[11] Ted J. Jansen, Solar Engineering Technology, Englewood Cliffs, New Jersey, U.S.A. (1985).

[12] Frederick F. Simon, Flat plate solar collector performance evaluation with a solar simulator as a basis for collector selection and performance prediction, Journal of Solar Energy, Vol. 18, pp. 451-466, 1976.

[13] Duffie, J.A., Beckman, W.A., Solar Engineering of Thermal Processes, 2nd edition. John Wiley, New York, U.S.A. (1991).

[14] Nafey, A.S., Design and simulation of seawater-Thermal desalination plants", Leeds University, Ph.D. Thesis, 1988.

[15]] Al-Ajlan, S.A., Al Faris, H., Khonkar, H., A simulation modeling for optimization of flat plate collector design in Riyadh, Saudi Arabia, Journal of Renewable Energy, Vol. 28, pp. 1325-1339, 2003.

[16] Nafey, A.S., Mohamad, M.A., El Helaby, S.O., Sharaf, M.A., Statistical Evaluation of Some Models for Estimation of Instantaneous Direct and Diffuse Insolation on Horizontal Surfaces in Suez Gulf Region-Egypt, to be published.

APPENDIX A

A.1. The error analysis of the experimental work

The measured experimental data includes some errors due to the uncertainty of the measuring process and the limited precision of the experimental instruments. For the examination of the validity of the experimental work; the following fractional error (*Fr*) equation is used:

$$\%Fr = \frac{Calculated - Measured}{Calculated} \times 100$$

The average *Fr* percentage for the measuring of the solar radiation was about 1%-2%. For the TBT; the *Fr* error; was not exceeding about 6%-7%. Also for the wasted brine and outlet feed water temperatures; the percentage was about 9% and 8% respectively. The percentage for the system performance ratio PR is about 4% and 9% for the system productivity DP.

Table A-1 The *Fr* error percentage of the measured data

Parameter:	***Fr* Percentage%:**
I_S	2%
TBT	6%-7%
T_{b1}	9%
T_{icol}	8%
DP	9%
PR	4%